Desalination and Water Treatment
www.deswater.com

doi: 10.1080/19443994.2015.1129649

57 (2016) 22341–22352
October

Taylor & Francis
Taylor & Francis Group

Activated coconut coir for removal of sodium and magnesium ions from saline water

Eshani Hettiarachchi[a], Rumali Perera[b], A.D.L. Chandani Perera[a,*], Nilwala Kottegoda[c,d]

[a]*Department of Chemistry, University of Peradeniya, Peradeniya, Sri Lanka, Tel. +94 773594127; emails: kiyashaeshanie@gmail.com (E. Hettiarachchi), chandanip@pdn.ac.lk (A.D.L. Chandani Perera)*
[b]*Mahamaya Girls College, Kandy, Sri Lanka, email: rum_tr@yahoo.com*
[c]*Department of Chemistry, University of Sri Jayewardenepura, Nugegoda, Sri Lanka, email: nilwala@sjp.ac.lk*
[d]*Centre for Excellence in Nanotechnology, Nanoscience and Technology Park, Sri Lanka Institute of Nanotechnology, Pitipana, Homagama, Sri Lanka*

Received 11 July 2015; Accepted 2 December 2015

ABSTRACT

The potential of laboratory-prepared-activated coconut coir (ACC) for removal of Na^+ and Mg^{2+} ions from saline water in desalination applications was studied. ACC was prepared by pyrolysis of raw coconut coir dust, treated with 50 wt% phosphoric acid. The ACC was characterized by Fourier transform infrared spectroscopy, powder X-ray diffraction, and scanning electron microscopy techniques while its BET surface area, methylene blue, and iodine values were measured to understand the surface characteristics. The laboratory-prepared-activated coir demonstrated a nanoporous structure with a BET surface area of $1,235\ m^2\ g^{-1}$. The results further indicated the presence of oxygen containing functional groups in weak graphitic structure, while micro- to nanoporous nature was observed in ACC. Na^+ and Mg^{2+} ion removal efficiencies from standard $0.200\ mol\ dm^{-3}$ NaCl and $MgCl_2$ solutions were found to be approximately 50%. The results fit into Langmuir and Freundlich isotherms implying homogeneous monolayer coverage for both Na^+ and Mg^{2+} adsorption. Optimized ACC dosage for removal of 40% of both cations from seawater was found to be $80.0\ g\ L^{-1}$. ACC has the potential to remove up to 80% of Na^+ and 72% of Mg^{2+} from seawater by repeated filtration. The acidic point zero charge of 5.5 ± 0.1 and the presence of nanopores explain the high cation adsorption characteristics compared to commercially available activated carbon. The used ACC was successfully regenerated by back washing with distilled water followed by pyrolysis.

Keywords: Desalination; Activated coconut coir; Pyrolysis; Saline water; Na^+; Mg^{2+} removal efficiency

---

1. Introduction

An adequate supply of safe drinking water is one of the major prerequisites for a healthy life, while the extent of access to clean water resources is a parameter ensuring that human basic needs are met. Although over 70% of the earth's surface is covered by water, most of it is unavailable for human consumption. Over 30% of the freshwater is locked up in ice caps and glaciers while 20% is inaccessible.

---

*Corresponding author.

Freshwater lakes, rivers, and underground aquifers represent only 2.5% of the world's total freshwater supply. Unfortunately, in addition to being scarce, freshwater is also very unevenly distributed [1]. The United Nations Organization has compared water consumption with its availability and has predicted that by the middle of this century between 2 and 7 billion people will live with water scarce or water-stressed conditions [1]. According to the predicted water scarcity map, in the twenty-first century, many countries are entering an era of severe water shortage, increasing competition among agricultural, industrial, and domestic users leading to significant increases in the real cost of water. As a result, water will become the oil of twenty-first century, which may even lead to armed conflicts among the nations.

Many countries already face the problem of finding water with good quality for consumption. Use of seawater, which is the largest water body on the planet, is one of the future solutions for predicted water related issues [2]. There had been many attempts to implement desalination methods to use seawater for human consumption. The major desalination technologies currently in practice are membrane separation via reverse osmosis and thermal distillation. However, both these techniques are of high cost and therefore, lacks of environmental and economic sustainability [3,4]. Conventional thermal desalination processes are inefficient in their use of energy, while corrosion effects have further limited its practical use while reverse osmosis use electrical energy, which is of high cost leading to drawbacks in large-scale implementations, where energy is a scarce resource.

Many studies towards developing more efficient methods of desalination have been focused on exploring cheap energy sources such as solar energy for the above listed methods [5,6]. On the other hand, attempts have also been made to develop desalination methods based on new technologies such as nanotechnology, however most of these developments are in early stage while the major drawback being the high cost involved in developing the materials. For example, functionalized graphene sheets have been used in desalination applications [7].

However, only few attempts have been reported on exploration of low-cost materials for desalination applications. For example, Gascó et al. have studied the use of sewage sludge pyrolyzed carbon for removal of Mg^{2+}, Ca^{2+}, Na^{+}, and K^{+} [8], while Dassanayake and co-workers have reported the use of natural clay for removal of cations from saline water [9]. Therefore, there is an increased scientific interest to explore cheap desalination techniques.

Activated carbon (AC) known as the oldest adsorption material has a porous structure which gives a large surface area ranging from 500 to 2,000 $m^2 g^{-1}$. As a result, AC is widely used in removal of organic pollutants, pathogens, and heavy metals from drinking water and industrial effluents [10–13]. However, it has not been studied on potential use of AC in desalination applications.

Theoretically, any carbonaceous material can potentially be activated chemically or physically to obtain AC. In the old days, the most commonly used raw materials were coal, coconut shells, wood, and peat, while, recently, natural raw materials such as bamboo, rice-husk, walnut shells, peach pits, saw dust, coconut coir, and palm kernels have been used in making AC. Depending upon the raw material and the method of activation, the properties of AC will obviously be variable [14,15].

Coconut coir dust, a natural fiber obtained from the coconut husk, is one of the potential candidate for the synthesis of AC. Coconut coir fibers are bound together through lignin, natural polymer, and the second most abundant phenolic polymer which cements the fibers together. Coir dust, removed during the extraction of coir fiber from coconut husk, is a waste biomass, readily available and a cheap material in coconut fiber industry in Sri Lanka and other tropical countries. However, only few studies on synthesis and use of AC based on coconut coir have been reported to date. For example, activated coconut coir (ACC) has been used as electrode materials for desalination applications based on electrochemical approach and for organic dye removal [13,16,17]. Perera et al. have carried out the preliminary studies on the efficiency of cation removal using commercially available activated coir [18]. Further to this preliminary work by Perera and co-workers this study focuses on the potential use of laboratory-prepared-ACC dust for desalination applications in domestic level.

The ACC was prepared by chemical activation using H_3PO_4 acid as activating agent followed by pyrolysis. Morphological characterization was performed by scanning electron microscope (SEM) and X-ray diffraction (XRD), while structural characterization by X-ray fluorescence (XRF) and Fourier transform infrared (FTIR) spectroscopy. The adsorption characteristics were studied by determining iodine and methylene blue values. The removal of Na^{+} and Mg^{2+} cations from aqueous medium was initially studied using standard solutions and subsequently used natural seawater. Further, equilibrium adsorption studies based on Langmuir, Freundlich, Temkin, and DRK were carried out to understand the nature of adsorption process taking place during removal of these cations. Energy saving and highly efficient regeneration method was explored to reuse ACC repeatedly. The study was conducted at room temperature in dynamic batch method to be representative of environmentally relevant and practically attainable condition.

2. Materials and methods

2.1. Materials

All chemicals used were of analytical grade and purchased from BDH Chemicals Ltd. Unless otherwise indicated, all chemicals were used as received. All solvents were distilled prior to use. metal ion salts of NaCl (99 wt% assay) and $MgCl_2$ (99 wt% assay) were used without further purifications. Distilled water was used for standard solution preparation.

Raw coconut coir dust was collected from Rambukkana, Sri Lanka while seawater was collected from Kalutara, Sri Lanka.

2.2. Instrumentation

FT-IR spectroscopic analysis was done using FT-IR (IR- PRESTISE -21, SHIMADZU) spectrophotometer using KBr method in the range of 400–4,000 cm^{-1}. XRF studies were carried out using the XRF spectrophotometer (Fischerscope Model-DF500FG-456). XRD studies were carried out using a Brucker D8 focus X-ray powder diffractometer using Cu Kα radiation (wavelength—1.540 Å) over a 2θ range from 2˚ to 70˚ with the step size of 0.02˚. scanning electron microscopy (SEM) analysis was conducted using Hitachi SU 6600 SEM using the secondary electron mode. All the samples were gold coated prior to analysis. The concentrations of Na^+ and Mg^{2+} ions were measured using BUCK Scientific Atomic Absorption spectrophotometer AAS 200-A. Calibration curves were constructed using standard samples for determination of unknown concentrations. BET surface area analysis was carried out using Quantachrome® ASiQwin™ instrument.

2.3. Preparation and characterization of ACC

Coconut coir dust was thoroughly washed and dried at 100˚C in an oven for 24 h. After drying the adsorbent was sieved to obtain particle sizes less than 1,000 μm. Then, 30.00 g of dried coir dust was soaked in activating agent, H_3PO_4 acid, (1.000 mol dm^{-3}, 50 wt%), boiled for 1 h and kept in an oven at 100˚C for 48 h. Then it was pyrolyzed at 450˚C for 1 h, cooled down to room temperature and washed repeatedly with distilled water until the pH 7 was reached in the supernatant. This assures removing of any remaining phosphoric acid from the product. It was oven dried at 100˚C for 48 h before use. The phosphoric acid used was recovered after the activation stage and was reused.

2.4. Adsorption characteristic of ACC

2.4.1. Iodine value test

The iodine number, defined as the amount ofi odine (mg) that is adsorbed by 1 g of adsorbent at an equilibrium concentration, was measured according to the procedure established by the American Society for Testing and Materials (ASTM 2006) [19].

Three samples of ACC of masses 0.500, 1.000, and 1.500 g were placed in Erlenmeyer flasks equipped with stoppers. Then, 10.00 ml of 5% (w/v) hydrochloric acid solution was added to each flask and swirled the solution gently until the ACC sample was completely wetted. The contents were brought to boil for 30 s to remove any sulfur present and cooled down to room temperature. Then, 50.00 ml of 0.100 mol dm^{-3} iodine solution was added to each flask, vigorously shaken for 30 s and quickly filtered. The filtrate was titrated with standard 0.100 mol dm^{-3} sodium thiosulphate solution. The iodine value of synthesized ACC sample was calculated and it was compared with that of the commercially available AC.

$$\text{Iodine number} = \frac{\text{mass of iodine consumed/mg}}{\text{mass of activated coir/g}} \times 100 \tag{1}$$

2.4.2. Methylene blue test

Methylene blue number is a parameter used in characterization of AC. It provides an indication of decoloring properties of AC (sorption properties in solution).

First, (1.500 g) of synthesized ACC was added to a 100 ml beaker. Then, 25.00 cm^3 of methylene blue solution (1,000 ppm) was added to it and the mixture was stirred with a mechanical stirrer for 5 min at a speed of 500 rpm. The mixture was filtered through glass wool in a funnel. The absorption of filtrate was measured at 662 nm using a UV–vis spectrophotometer. Then, the MB adsorption value was calculated and compared with that of the commercial AC [17].

$$\text{Methylene blue number} = \frac{\text{Amount of the dye adsorbed/mg}}{\text{Mass of the activated coir used/g}} \quad (2)$$

2.4.3. BET surface area analysis

Powdered sample (27.6 mg) was subjected to degassing at 673 K for overnight (~3 h) prior to the analysis. All samples were oven dried at 150˚C before degassing. After the degassing, microphore analysis was conducted for 48 h.

2.5. Morphological and structural characterization

The FTIR spectra of raw coconut coir and ACC samples were recorded in the range of 400–4,000 cm^{-1} using KBr method. XRF spectrum of ACC was recorded to find out the presence of heavy metals in the sample. The functional group characteristics of the ACC was studied using FTIR spectroscopy while the presence of heavy metals in the final product was investigated by XRF technique. The crystallinity and the nature of the crystalline structure were studied using Powder X-ray diffraction (PXRD) method. The morphological characteristics have been understood using SEM.

2.6. Cation removal capacity

2.6.1. Time optimization and mass optimization

The synthesized ACC was thoroughly washed with distilled water until the supernatant pH reached 7, to remove excess H_3PO_4, oven dried for 24 h and sieved to get particles less than 500 μm in size. Initially, time optimization (stirring time and settling time) and mass optimization were carried out with standard samples.

ACC (0.50 g) was added into a 100 cm^3 beaker and 50.00 cm^3 of 0.200 mol dm^{-3} NaCl was added to it. The mixture was stirred with a mechanical stirrer for 5 min at 300 rpm and allowed to equilibrate for 15 min followed by filtering through a sintered glass crucible. The solutions were diluted and the equilibrium concentration of Na^+ in the filtrate was determined using an AAS at 589 nm and a calibration plot. The procedure was repeated for different stirring times and settling times (10, 15, 20, 25, and 30 min). The mass optimization was also carried out by varying ACC mass from 0.50 to 4.00 g in 0.50 g mass intervals. The procedure was repeated for 0.200 mol dm^{-3} $MgCl_2$ solution.

2.6.2. Effect of initial cationic concentration

The effect of initial cation concentration on the cation removal was studied at different concentrations of standard solutions using optimized times and mass of ACC. A series of standard solutions of NaCl (0.200, 0.300, 0.400, 0.500, 0.600, 0.700, 0.800, 0.900, and 1.000 mol dm^{-3}) was prepared. Then, ACC (1.50 g, optimized mass) was placed in a beaker and 50.00 ml of 0.200 mol dm^{-3} of NaCl solution was added, stirred with a mechanical stirrer at a speed of 500 rpm for 20 min (optimum stirring time) and was equilibrated for 15 min (optimum settling time) followed by filtering. The equilibrium concentration of sodium ions in the filtrate was obtained using AAS at 589 nm. The same procedure was followed for the other concentrations of the NaCl solutions. The above procedure was repeated for $MgCl_2$ standard solutions. Concentrations of Mg^{2+} ions in filtrates were obtained using AAS at 285 nm.

2.6.3. Adsorption capacity of ACC for Na^+ and Mg^{2+} in seawater

Seawater sample collected from Kalutara, Sri Lanka, was used in the analysis. Physical parameters of seawater such as pH and conductivity were initially measured. Initial concentrations of Na^+ and Mg^{2+} were also measured using AAS. Different masses of ACC (0.50, 1.00, 1.50, 2.00. 2.50, 3.00, 4.00, 4.50, and 5.00 g) were placed in beakers and 50.00 ml of seawater sample was added to each beaker and stirred with a mechanical stirrer for 20 min at a speed of 500 rpm. The solutions were equilibrated for 15 min followed by filtering through a sintered crucible. Concentration of Na^+ and Mg^{2+} in the filtrates was determined using AAS at 589 nm and 285 nm, respectively.

Repeated treatment of the seawater by ACC was carried out (up to 10 times) in order to improve the efficacy of the system.

2.7. Point of zero charge determination (pzc)

The pzc value was determined for each synthesized ACC and commercial-activated charcoal using simplified mass potentiometric titration method.

First, two identical solutions (blank and sample) were prepared with 3.00 cm^3 of 0.100 mol dm^{-3} KNO_3 and 6.00 cm^3 of distilled water, and their pH values were recorded. Then, 1.00 cm^3 of 0.010 mol dm^{-3} KOH was added to the blank solution and the pH was recorded again. 50.00 mg of synthesized ACC was then added to the sample solution, followed by addition of 1.00 cm^3 of 0.010 mol dm^{-3} KOH solution. Then, pH titration was carried out for both blank and sample with 0.010 mol dm^{-3} HNO_3 and the variation of pH with the volume of HNO_3 solution was plotted. The pzc of the sample was estimated at the point where both titration curves crossed each other. The pH value at the cross-over point is the pzc value of the adsorbent. The same procedure was followed for the 50.00 mg sample of commercial-activated charcoal.

2.8. Regeneration of used ACC

The used ACC was stirred in 50 ml of distilled water at the speed of 500 rpm for 20 min. This procedure was repeated for five times. The washed sample was then dried in an oven at 50°C for 24 h. Then, one portion of the sample was treated with conc. HCl acid solution (50.00 ml) and stirred for 20 min at 500 rpm. Other portion of the sample was pyrolyzed at 300°C for one hour. Then, each regenerated sample was characterized using methylene blue adsorption capacity. The efficiency of cation removal of regenerated ACC was tested using 0.200 mol dm^{-3} $MgCl_2$ solution.

2.9. Resistance to microbial attack

As the activated product has to be used in water filters resistance to microbial attack in water and saline water was tested. Both filtrates and used ACC were kept aside and observed for microbial growth up to 60 d.

All experiments in the study were triplicated.

3. Results and discussion

The objective of this project was to synthesize and characterize AC prepared from naturally abundant coconut coir dust and study the potential of using them for the removal of Na^+ and Mg^{2+} cations from the seawater or lagoon water in order to develop a low-cost desalination method. AC is well known for its high surface area, porosity and adsorption characteristics which are originated from the electronic states of the surface atoms, concentration of the foreign ions and type of defects, presence of functional groups, voids, and interstitials.

The activation process of raw coir by phosphoric acid occurs in several steps. First, the wetting of raw coir by phosphoric acid initiates a reaction between the acid and the lignin functional groups. In the presence of phosphoric acid, lignin undergoes cleavage of aryl ether bonds, which is resulting in the formation of ketone groups, while CO and CO_2 are released as volatile products leading to formation of a porous structure [20].

3.1. Morphological and structural characterization of ACC

The prepared ACC was characterized by BET analysis, methylene blue, and I_2 absorption capacity tests, FT-IR spectroscopy, PXRD, XRF, and SEM. The adsorption characteristics of ACC were studied by determining iodine value and methylene blue value and comparing them with those obtained for commercial AC. BET analysis confirmed a surface area of 1,235 m^2/g for ACC suggesting its potential applications in various fields as for commercial AC.

As indicated by the data in Table 1 both iodine value and methylene blue adsorption capacity are higher for laboratory prepared ACC than those of commercial AC. Hence, significantly higher adsorption capacity is expected in the laboratory-prepared-ACC product.

3.1.1. FT-IR characterization

Structural characteristics were studied using the FT-IR spectroscopy. Fig. 1 compares the FT-IR spectra of raw coconut coir and ACC.

Table 2 presents all major peak positions observed in FT-IR spectra of raw coconut coir and ACC.

As expected the vibrations related to the lignin-based polymeric materials particularly those related to phenolic and methoxy, alkene, and alkane type groups are observed in the raw coir. After activation process new functional groups such as carboxylate, and phosphate have appeared while the –OH stretching frequency has slightly shifted to a lower wave number suggesting the formation of a strong H-bonding network possibly due to the new functional groups. The peaks due to the aromatic ring vibration have disappeared after phosphate activation suggesting the destruction of lignin type ring structure.

3.1.2. PXRD analysis

The PXRD pattern of synthesized ACC sample in Fig. 2 shows a peak at an angle (2θ) of 24° corresponding to an interlayer spacing of 0.35 nm and this could be attributed to the hexagonal graphitic carbon structure (0 0 2 plane) [21]. This peak provides evidence to confirm the transformation of the polymeric coconut coir into graphitic carbon. The low intensity and broadness of the observed peak suggest an amorphous structure for the synthesized ACC.

Table 1
Iodine value and methylene blue adsorption value of laboratory prepared ACC and commercial AC

ACC type	Iodine value/(mg g^{-1})	Methylene blue value/(mg g^{-1})
Laboratory prepared ACC	601	331
Commercial activated carbon	593	106

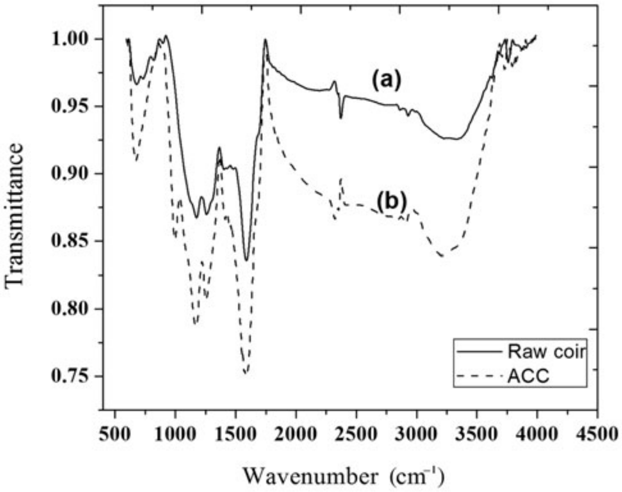

Fig. 1. FT-IR spectra of (a) raw coconut coir and (b) activated coconut.

3.1.3. SEM and XRF characterization

As observed by the SEM image in Fig. 3 the ACC possess porous structural features. The pores are in the nanometer size scale. Presence of nanometer size pores will introduce higher adsorption capacity into the ACC material. In addition, the graphitic-like layered structure is observed in the internal structure suggesting a successful pyrolysis process converting ligno-cellulose into graphitic carbon.

Furthermore, XRF analysis suggested the absence of any heavy metal in the final product.

3.2. Cation removal capacity

The percentage removal of cations from aqueous solution by ACC was calculated using the following equation:

$$\text{Removal}\,(\%) = \frac{C_0 - C_e}{C_0} \times 100 \qquad (3)$$

where C_0 is the initial concentration (ppm) and C_e the equilibrium concentration (ppm) of cations.

The effect of contact time on the removal of cations was investigated by varying the stirring time and settling time allowing sufficient time to achieve adsorption equilibrium in the adsorbant/aqueous cation system. The effect of dosage of adsorbant on the removal of cations from aqueous solution was studied by varying the mass of ACC. The maximum percentage removal of both Na^+ and Mg^{2+} was obtained at the optimum stirring time of 20 min and settling time of 15 min with 1.5 g of ACC. In order to understand

Table 2
Interpretation of FT-IR spectra of raw coconut coir and ACC

Raw coir		ACC	
Wavenumber/cm^{-1}	Functional group assignment	Wavenumber/cm^{-1}	Functional group assignment
3,870–3,270	–OH stretching	3,800–3,220	–OH stretching
2,700–2,800	C–H stretching of lignin type polymers	2,700–2,800	C–H stretching of lignin type polymers
1,580	Alkene type C=C stretching	1,590	Carboxylate asymmetric stretching
1,265	C–CH_3 stretching and ring stretching, O–H phenolic	1,430	Carboxylate symmetric stretching
1,170	Aliphatic ethers asymmetrical stretching and O–H alcoholic	1,250	Aromatic ring vibrations and C–CH_3 stretching
700	C–OH out of plane bending	1,170	Aliphatic ethers asymmetrical stretching and O–H alcoholic
		995	Phosphate stretching
		680	Aromatic ring vibrations

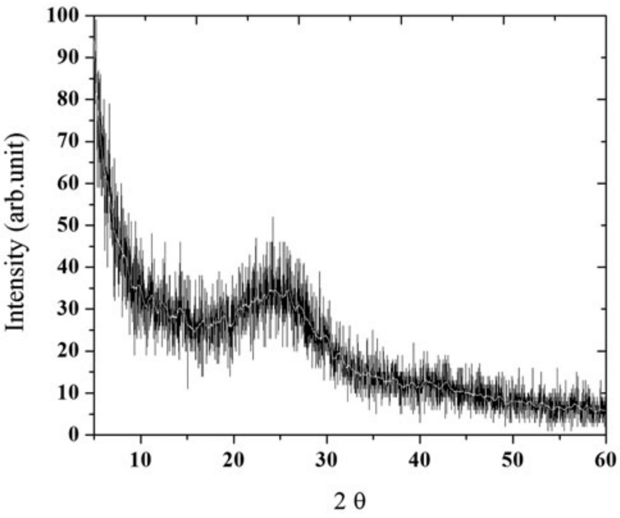

Fig. 2. Powder X-ray diffractions pattern of synthesized ACC.

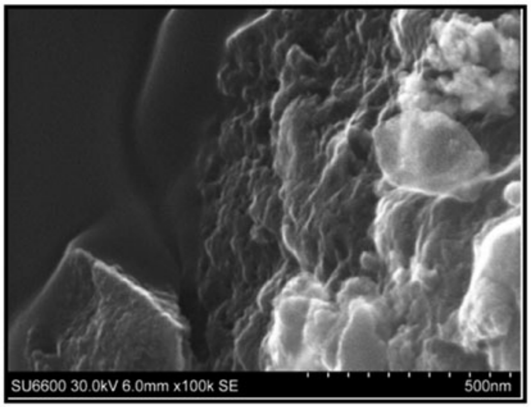

Fig. 3. SEM image of ACC.

the adsorption capacity of synthesized-ACC, removal of Na^+ and Mg^{2+} from standard solutions of NaCl and $MgCl_2$ were first studied.

The equilibrium adsorption capacity of ACC (Q) was calculated as:

$$Q = \frac{V(C_0 - C_e)}{m} \tag{4}$$

where V is the volume of adsorbate (dm^3), C_0 and C_e are the initial and equilibrium concentrations of adsorbate (ppm), and m the mass of dry adsorbent (g).

The equilibrium adsorption capacity (Q) calculated using the Eq. (2) for both cations at different initial concentrations of salt solutions, are given in the Table 3. The equilibrium adsorption capacity increases with the initial concentration of salt solutions for both cations. The process of removal of cations through adsorption depends on the concentration gradient between the adsorbate and the initial concentration of cations. Therefore, at low concentrations of cations in the medium this adsorption–desorption equilibrium state is reached faster thus leading to low-adsorption capacity. This dependency is more prominent particularly if the adsorption is a monolayer coverage.

Fig. 4 represents the variation of percentage removal of both cations as a function of initial concentration of salt solutions. As indicated in the Fig. 4, at high concentrations of cations (1.000 mol dm^{-3}) 50–60% removal of both Na^+ and Mg^{2+} ions were observed when 50.00 ml of salt solutions were treated with 1.50 g of ACC. For high-concentrated solutions a fast adsorption–desorption equilibrium state within 20 min was achieved suggesting the potential for use of ACC in future desalination applications.

3.3. Adsorption equilibrium studies of ACC

Langmuir, Freundlich, Temkin, and DRK isotherm studies were carried out to understand the nature of adsorption process taking place during removal of these cations.

3.3.1. Langmuir isotherm

Langumuir isotherm is a semi-empirical formula derived from statistical thermodynamics with kinetic basis for gases/liquids adsorbed to solid adsorbents:

$$q_e = K_L Q^0 C_e / (1 + K_L C_e) \tag{5}$$

Rearranging the above Eq. (3) to obtain a linear form:

Table 3
Equilibrium adsorption capacity for Na^+ and Mg^{2+}

Initial salt concentration/mol dm^{-3}	Q/mg g^{-1}	
	Na^+	Mg^{2+}
0.100	76.9	45.7
0.200	117.6	86.6
0.300	154.2	130.0
0.400	188.8	167.6
0.500	240.8	208.1
0.600	291.5	267.5
0.700	325.5	303.7
0.800	359.0	378.3
0.900	416.3	481.3

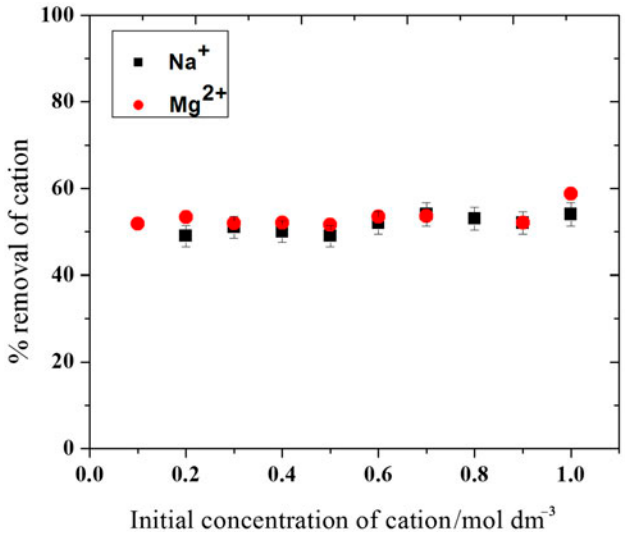

Fig. 4. Dependence of % removal of Na^+ and Mg^{2+} with the initial concentrations of salt solutions.

$$\frac{1}{q_e} = \frac{1}{K_L Q^0 C_e} + \frac{1}{Q^0} \tag{6}$$

where, q_e (mg g^{-1}) and C_e (mg L^{-1}) are the amounts of adsorbed metal ion per unit mass of adsorbent and unadsorbed metal ion concentration in adsorbate solution at equilibrium, respectively. The constant K_L is the Langmuir equilibrium constant and Q^0 is the maximum monolayer adsorption capacity. The Eq. (4) describes quantitatively the formation of a monolayer adsorbate on the outer surface of the adsorbent, and after monolayer adsorption is complete no further adsorption takes place. It is valid for monolayer adsorption onto a surface containing a finite number of identical sites and assumes uniform energies of adsorption onto the surface.

As shown in Fig. 5(a) and (b) experimental results obtained for Na^+ and Mg^{2+} ions fit well to the Langmuir isotherm, Eq. (4), with higher r^2 vales even at moderately high concentrations of cations. The adsorption of both cations by ACC implies a monolayer coverage obeying Langmuir isotherm. The Langmuir isotherm constants for both Na^+ and Mg^{2+} are summarized in Table 4. The monolayer adsorption capacity calculated from Langmuir isotherm is higher for Mg^{2+}adsorption than that of Na^+ ions.

3.3.2. *Freundlich isotherm*

The Freundlich isotherm is purely an empirical formula representing the isothermal variation of adsorption of a quantity of gas adsorbed by unit mass of solid adsorbent with pressure or a quantity of any species in solution phase adsorbed by unit mass of solid adsorbent as a function of concentration given by:

$$q_e = K_F\, c_e^{\frac{1}{n}} \tag{7}$$

Rearranging above Eq. (5), a linear form is obtained:

$$\log q_e = \frac{1}{n} \log C_e + \log K_F \tag{8}$$

where K_F is the Freundlich constant which relates to adsorption capacity and n is the Freundlich exponent, which relates to adsorption intensity. K_F and n can be

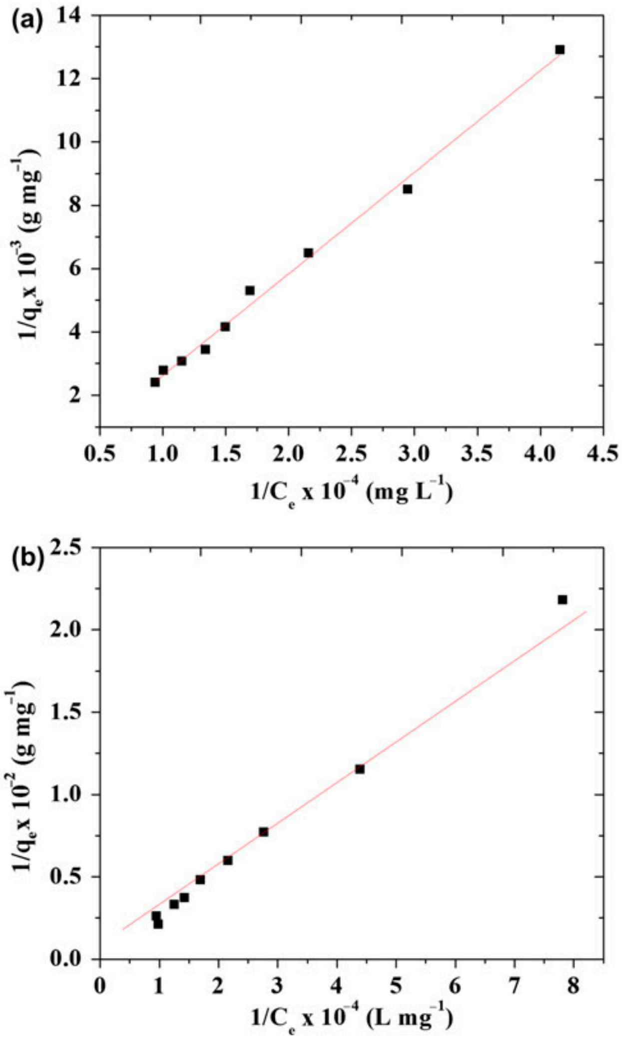

Fig. 5. Langmuir adsorption isotherm for (a) Na^+ removal and (b) Mg^{2+} removal.

Table 4
Constants of Langmuir and Freundlich adsorption isotherms

Cation	Langmuir isotherm			Freundlich isotherm		
	$K_L/(\text{dm}^3\ \text{g}^{-1})$	Q^0 (mg g^{-1})	r^2	$K_F/(\text{mg g}^{-1})$	n	r^2
Mg^{2+}	4.77×10^{-5}	743.4	0.9979	38.90	0.948	0.9995
Na^+	6.88×10^{-5}	454.5	0.9999	70.80	0.895	0.9868

calculated using a plot of log q_e vs. log C_e. Freundlich isotherm is commonly used to describe adsorption characteristics in a heterogeneous surface.

Fig. 6(a) and (b) illustrate a linear fit of experimental results obtained for Na^+ and Mg^{2+} ions to the Freundlich adsorption isotherm, with higher r^2 values, even at moderately higher concentrations of cations. Table 4 summarizes Freundlich adsorption isotherm constants. This observation further implies a monolayer process on the adsorbate.

The adsorption of both cations does not obey linear form of Temkin and DRK adsorption isotherms confirming the multi-layer adsorption does not take place.

The Langmuir isotherm is based on the assumption that the monolayer adsorption onto a surface containing finite number of identical adsorption sites. It also, assumes the sites have uniform force toward the adsorbate and no migration of adsorbate occurs during the process in the plane of surface.

Linear fit of the experimental data into Langmuir isotherm model indicates the formation of a monolayer coverage of cations at the outer surface of ACC.

On the other hand, the Freundlich isotherm model assumes heterogeneous adsorption in which the energy term in the Langmuir equation varies as a function of the surface coverage.

In Freundlich equation, K_F and n are Freundlich constants, where n gives an indication of how favorable the adsorption process is and K_F gives the adsorption capacity. The linear form of Freundlich isotherm has been widely applied to correlate sorption data where $1/n$ is a heterogeneity parameter. The smaller the $1/n$ value, the greater the expected heterogeneity.

The value of $1/n$ below one indicates normal Freundlich adsorption behavior while above one is indicating a collective adsorption. If n is between 1 and 10 usually the adsorption is favorable.

As shown in Table 4, the value of $1/n$ for magnesium ion is 1.05 and that for sodium ion is 1.1.

We can consider that both Mg^{2+} and Ca^{2+} show normal Freundlich adsorption on ACC surface.

Thus, for an equilibrium concentration of 1 mg dm^{-3} of cation in aqueous solution, one gram of ACC can remove 38.90 mg of Mg^{2+} and 70.80 mg of Na^+ at room temperature of 298 K.

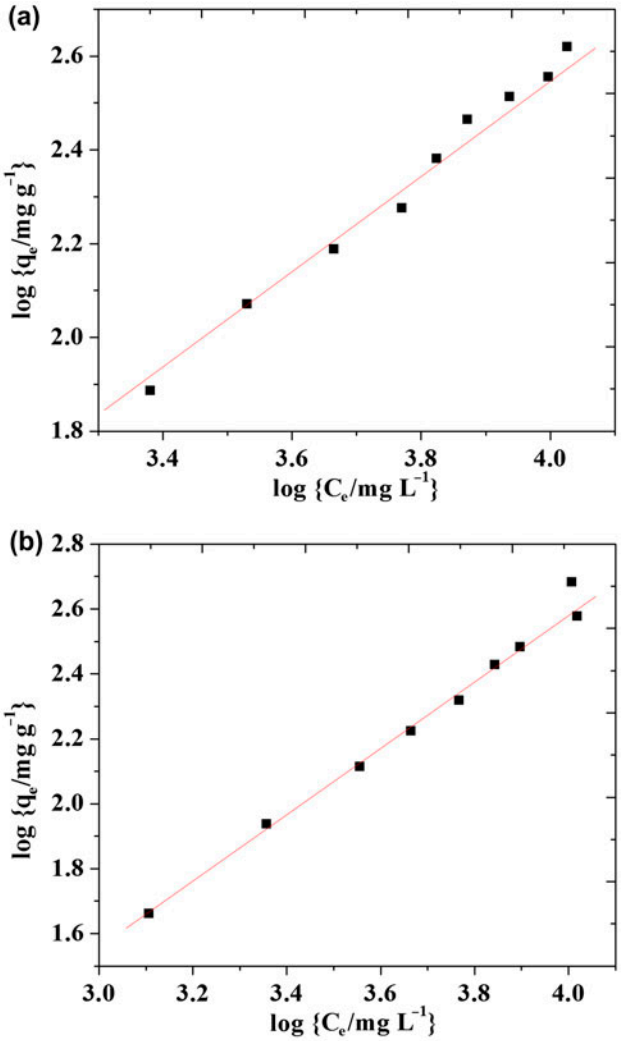

Fig. 6. Freundlich adsorption isotherm for (a) Na^+ removal and (b) Mg^{2+} removal.

3.4. Cation removal capacity of ACC from seawater

Natural seawater samples obtained from Kalutara, Sri Lanka, has been used in the next step of study. Some of the physical parameters of natural seawater sample are tabulated in Table 5.

Table 5
Physical parameters of seawater

Parameter	Quantity
pH	8.5
Conductivity/S	4.912×10^{-2}
Color	Clear
$[Na^+]$/ppm	10,597
$[Mg^{2+}]$/ppm	1,257

3.4.1. Removal efficiency of Na^+ and Mg^{2+} ions from seawater with different masses of ACC

Optimization of the mass against the cation removal efficiency was carried out using different masses of ACC for 30.00 ml of the seawater sample. Fig. 7 illustrates the variation of % removal of Na^+ and Mg^{2+} with the amount of ACC used.

According to the AAS results it was found that the initial amount of Mg^{2+} and Na^+ present in seawater was 1,257 and 10,597 ppm, respectively. When the seawater was allowed to be in contact with ACC a maximum removal of 35% for both cations was obtained for 4.0 g of ACC. The equilibrium adsorption capacities deduced from Eq. (2) for the removal of Na^+ and Mg^{2+} cations from seawater are summarized in Table 6. The maximum adsorption capacity of 43.7 and 5.5 mg g^{-1} was obtained for Na^+ and Mg^{2+} ions, respectively, from seawater when 4.0 g of ACC was used.

Repeated filtration studies were carried out for both cations using 4.00 g of ACC for 50.00 ml seawater samples in order to improve the cation removal efficiency. The percentage removal of both cations increases with the increase in number of repeated filtrations as shown in Fig. 8.

In this experiment it was observed that the Na^+ concentration drops from 10,597 to 2,116 ppm after 10 repeated filtrations (80% removal), while the Mg^{2+}

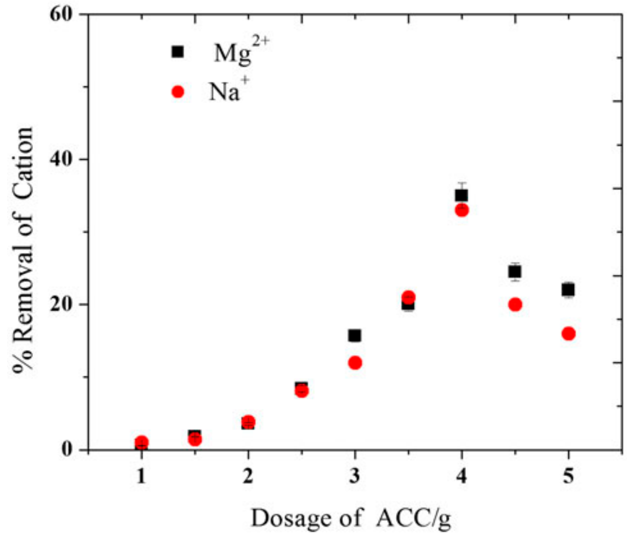

Fig. 7. Dependence of percentage removal of Na^+ and Mg^{2+}on the amount of ACC used.

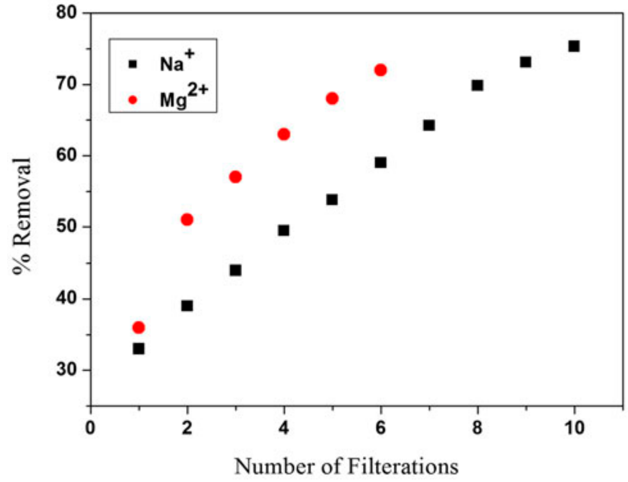

Fig. 8. Percentage removal of cations upon repeated filtrations for Na^+ (■) and Mg^{2+} (●) in seawater.

Table 6
Adsorption capacity of Na^+ and Mg^{2+} in seawater with different ACC amounts

Mass of ACC/g	Adsorption capacity for Na^+ in seawater/mg g^{-1}	Adsorption capacity for Mg^{2+} in seawater/mg g^{-1}
1.0	5.3	0.4
1.5	7.4	0.8
2.0	10.1	1.1
2.5	15.8	2.1
3.0	21.2	3.3
3.5	31.8	3.6
4.0	43.7	5.5
4.5	23.5	3.4
5.0	17.1	2.8

Table 7
Methylene blue adsorption and iodine values of regenerated and original activated coir samples

Sample	MB value/(mg/g)	Iodine value/(mg/g)	% Removal
ACC	333.28	601	53
RA—ACC	293.28	425	35
RP—ACC	332.87	598	52

concentration drops from 1,227 to 347 ppm after 5 filtrations (72%).

3.5. Point zero charge (pzc)

Point of zero charge (pzc) value for synthesized ACC is 5.5 ± 0.1, while that for commercially available AC is 7.9 ± 0.1.

The surface acidity of the adsorbent is important in understanding of the mechanism of adsorption reaction between ionic adsorbates and the adsorbent. The condition of a surface with no net charge is called point of zero charge (pzc). When solution $\mathrm{pH} > \mathrm{pzc}$ the surface of the adsorbent is predominantly negatively charged and hence, due to electrostatic interactions, cations adsorb onto the surface increasingly. When solution $\mathrm{pH} < \mathrm{pzc}$, the surface of the adsorbent is positively charged. Therefore, cations will have electrostatic repulsive forces with the surface which will decrease the adsorption [22]. The pH values of the tested solutions are greater than pzc of synthesized ACC. This explains the higher adsorption capacity of synthesized ACC towards the cations compared to the commercial AC with near neutral pzc. In addition, the nanoporous structure of the ACC further supports the higher adsorption capacity of ACC.

3.6. Regeneration of used ACC

The used ACC was first washed with distilled water and regeneration was carried out using two methods (i) acid treatment with HCl acid (RA-ACC) and (ii) pyrolysis at 300°C (RP-ACC). In order to understand the regeneration efficiency methylene blue adsorption and iodine value tests were carried out on both types of the regenerated ACC and, compared with the original ACC.

As evidenced by the results better regeneration efficiency was observed for the samples obtained after pyrolysis at 300°C. The ion removal efficiency for the regenerated ACC was also studied.

As expected, higher ion removal capacity of 52% was observed for RP-ACC as shown in Table 7. The percentage removal of Mg^{2+} ions from the original ACC and regenerated ACC by pyrolysis is similar to that of parent ACC.

It was noted that no microbial growth was observed in seawater filtered through either ACC or RP-ACC up to 60 d. Therefore, it can be concluded that both ACC and RP-ACC are resistance to microbial attack.

4. Conclusions

ACC can be synthesized with a high porosity and high ion removal capacity by treating coconut coir dust with 50 wt% phosphoric acid followed by pyrolysis at 450–500°C for 1 h. Compared to the AC production process this approach is much more energy efficient and less time consuming therefore, demonstrating the potential for applications in many areas. In this study, the laboratory-activated coir was tested for its desalination efficiency. The laboratory-ACC demonstrated high BET surface area (1,235 m^2/g) and nanoprorous structure with an acidic point zero charge. The experiments carried out with standard 0.200 $\mathrm{mol\,dm}^{-3}$ NaCl and MgCl_2 solutions demonstrated removal of about 50% of the cations after treating the solutions with 4.00 g of ACC for 20 min. The experiments were repeated with seawater containing 10,597 and 2,116 ppm Na^+ and Mg^{2+}, respectively. Single filtration through 4.00 g of ACC allowed to remove 35% of the cations. Repeated filtrations reduced Na^+ ions in seawater from 10,597 to 2,116 ppm (80% removal) and Mg^{2+} ions from 1,257 to 347 ppm (72% removal). More importantly, these used ACC were able to be regenerated using an easy path way by washing with water followed by pyrolysis using a gas stove at domestic level. The isotherm tests were conducted to understand the nature of the adsorption process. Results were in good agreement with the Freundlich and Langmuir isotherms implying a homogenous, monolayer coverage.

Acknowledgment

Authors acknowledge the Department of Physics, University of Peradeniya, Sri Lanka for providing facilities.

References

[1] M.A. Montgomery, M. Elimelech, Water and sanitation in developing countries: Including health in the equation, Environ. Sci. Technol. 41 (2007) 17–24.

[2] M.A. Shannon, P.W. Bohn, M. Elimelech, J.G. Georgiadis, B.J. Mariñas, A.M. Mayes, Science and technology for water purification in the coming decades, Nature 452 (2008) 301–310.

[3] Y. Zhou, R.S.J. Tol, Evaluating the costs of desalination and water transport, Water Res. 41 (2005) 1–10.

[4] S. Veerapaneni, B. Long, S. Freeman, R. Bond, Reducing energy consumption for seawater desalination, J. Am. Water Works Assoc. 99 (2007) 95–106.

[5] N. Hussain, A. Rahim, Utilization of new technique to improve the efficiency of horizontal solar desalination still, Desalination 138(1–3) (2001) 121–128.

[6] B. Van der Bruggen, Desalination by distillation and by reverse osmosis—Trends towards the future, Membr. Technol. 2003(2) (2003) 6–9.

[7] A.K. Mishra, S. Ramaprabhu, Functionalized graphene sheets for arsenic removal and desalination of sea water, Desalination 282 (2011) 39–45.

[8] G. Gascó, A. Méndez, J.M. Gascó, Preparation of carbon-based adsorbents from sewage sludge pyrolysis to remove metals from water, Desalination 1801–3 (2005) 245–251.

[9] T.M. Dassanayake, N. Kottegoda, A.D.L.C. Perera, Evaluation of ion adsorption capacities of Murunkan clay and coir as cost effective materials for desalination of water, Int. J. Earth Sci. Eng. 6(4) (2013) 788–790.

[10] I. Ghiloufi, L. Khezami, L.E. Mir, Nanoporous activated carbon for fast uptake of heavy metals from aqueous solution, Desalin. Water Treat. 55 (2015) 935–944.

[11] A. bin Jusoh, W.H. Cheng, W.M. Low, A. Nora’aini, M.J.M.M. Noor, Study on the removal of iron and manganese in groundwater by granular activated carbon, Desalination 182 (2005) 347–353.

[12] L. Monser, N. Adhoum, Modified activated carbon for the removal of copper, zinc, chromium and cyanide from wastewater, Sep. Purif. Technol. 26 (2002) 137–146.

[13] I.A.W. Tan, A.L. Ahmad, B.H. Hameed, Adsorption of basic dye on high-surface-area activated carbon prepared from coconut husk: Equilibrium, kinetic and thermodynamic studies, J. Hazard. Mater. 154 (2008) 337–346.

[14] F. Harry, F. Rodriguez-Rein, Activated Carbon, Elsevier Ltd., London, UK, 2004.

[15] P.J.M. Suhas, P.J.M. Carrott, M.M.L. Ribeiro Carrott, Lignin—From natural adsorbent to activated carbon: A review, Bioresour. Technol. 98 (2007) 2301–2312.

[16] B. Khalid, Qinghan Meng, R. Akram, B. Cao, Effects of KOH activation on surface area, porosity and desalination performance of coconut carbon electrodes, Desalin. Water Treat. (2014) 1–8.

[17] D. Kavitha, C. Namasivayam, Experimental and kinetic studies on methylene blue adsorption by coir pith carbon, Bioresour. Technol. 98 (2007) 14–21.

[18] T.R. Perera, S. Sellapperumage, T. Rathnayake, N. Kottegoda, A.D.L.C. Perera, Cost-effective method for reducing salinity in water, Proceedings of National Nanotechnology Conference, (2012), 142.

[19] American Society for Testing and Materials Standard Test Method of Determination of Iodine Number of Activated Carbon, ASTM Committee on Standards, (2006) 1–5.

[20] C. Namasivayam, D. Kavitha, Removal of Congo Red from water by adsorption onto activated carbon prepared from coir pith, an agricultural solid waste, Dyes Pigm. 54 (2002) 47–58.

[21] J.L. Gumaste, D. Satapathy, B. Mazumde, P.S. Mukherjee, B.K. Mishra, Preparation and characterization of activated carbon produced from coir pith waste, Indian Chem. Eng. 50(4) (2008) 288–300.

[22] M. Arlette, P. Cardenas, J.G. Ibanez, R. Vasquez-Medrano, Determination of the point of zero charge for electrocoagulation precipitates from an iron anode, Int. J. Electrochem. Sci. 7 (2012) 6142–6153.